THE SMALL-GAP UNDULATOR IMPEDANCE STUDY

M. Ivanyan[*], V. Tsakanov, CANDLE, Acharyan 31, 375040, Yerevan, Armenia

Abstract

The small gap undulator vacuum chamber resistive impedance is studied. The vacuum chamber is considered as a two-layer cylindrical tube with finite wall thickness. An analytical form of longitudinal impedance is obtained. The study includes both the thin and thick layer cases.

INTRODUCTION

The small gap undulators became an integrated part of advance synchrotron light sources. Therefore, its contribution to the broadband impedance of the ring is an important part to study the single bunch instability.

In this report, the longitudinal resistive impedance of two-layer pipe is studied that is modelling the small gap undulator impedance effect. The small gap undulator vacuum chamber inner surface is usually covered by thin film of special material with comparatively small conductivity (NEG) to provide high vacuum or with high conductivity (comparable with the main tube material) to reduce the resistive impedance of small aperture pipe. Vacuum chamber impedance is strongly depends on the cover material properties and thickness. The knowledge of the exact impedance induced by small gap indulator will allow to optimise the design of the chamber to obtain the required vacuum and to evaluate the real impedance of the ring. In Ref. [1] (see also citation there) a general algorithm to evaluate the coupling impedance of a plain uniform disk-like beam in a multi-layer, cylindrical vacuum chamber is given. The modification of this algorithm leads us to obtain the exact analytical expression for two-layer tube impedance.

THE PROBLEM

Consider the disk-like plain charge q (disk radius a_1) moving with velocity v along the uniform multi-layer cylindrical tube of inner radius a_2. The disk centre coincides with the tube axis. The boundary between two layers is located at $r = a_3$ and the outer radius of the tube is a_4 (Fig.1). Outside of the tube is a vacuum. The cross section of the tube is then divided into the five concentric regions: 1) $0 \le r \le a_1$, 2) $a_1 \le r \le a_2$, 3) $a_2 \le r \le a_3$, 4) $a_3 \le r \le a_4$ and 5) $r \ge a_4$. The frequency domain wave equation for longitudinal electrical component $\tilde{E}_z$ in each region can be written as:

$$\frac{1}{r}\frac{d}{dr}\left(r\frac{d\tilde{E}_z^i}{dr}\right) - \chi_i^2 \tilde{E}_z^i = -\frac{j\chi_i^2}{k\varepsilon_i}\tilde{\rho}_i, \quad i = 1,2,...5, \tag{1}$$

*ivanian@asls.candle.am

where $\tilde{\rho}_{i>1} = 0$ and $\tilde{\rho}_1 = q/c\pi a_1^2 \, e^{-jkz}$ is a charge density; in vacuum regions $\varepsilon_{1,2,5} = \varepsilon_0$ is a vacuum dielectric constant, in metallic layers $\varepsilon_i = \varepsilon_0 - j\sigma_i/\omega$, $(i = 3,4)$ with σ_i - the corresponding metal conductivity; ω is the frequency, χ_i are the radial propagation constants. In vacuum regions ($i = 1,2,5$) the radial propagation constants are given by $\chi_{1,2,5} = k/\gamma = \tau$ where γ is a Lorenz factor and $k = \omega/v$. In metallic layers the radial propagation constants are defined by the positive real part of

$$\chi_i = \sqrt{k^2/\gamma^2 + j\mu_0\sigma_i\omega}. \tag{2}$$
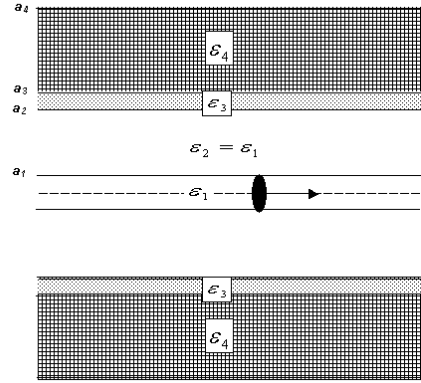

Figure 1. Geometry of the problem

SOLUTION

The tangential electrical field components may be presented in terms of the first and second order modified Bessel functions I_0, K_0. The longitudinal electrical field component in the beam region 1 is then read as:

$$\tilde{E}_z^{(1)}(r) = F_1 I_0(\tau r) + G_1 \tag{3}$$

with $G_1 = j\tilde{\rho}/k\varepsilon_0$.

In the subsequent regions 2,3,4 we have:

$$E_z^{(i)} = F_i R_i(r) + G_i S_i(r), \quad i = 2,3,4 \tag{4}$$

where

$$R_i(r) = K_0(\chi_i a_i) J_0(\chi_i r) - J_0(\chi_i a_i) K_0(\chi_i r) \tag{5}$$

$$S_i(r) = -K_1(\chi_i a_i) J_0(\chi_i r) - J_1(\chi_i a_i) K_0(\chi_i r)$$

In the outer region ($i = 5$) the field component is given by:

$$E_z = F_5 K_0(\tau r) \tag{6}$$

The coefficients F_i, $i=1,...5$ and G_i, $i=2,3,4$ are defined by the matching conditions at transition boundaries between two regions.

$$\begin{cases} \tilde{E}_z^{(i)}(\chi_i a_i) = \tilde{E}_z^{(i+1)}(\chi_i a_i) \\ \tilde{H}_\theta^{(i)}(\chi_i a_i) = \tilde{H}_\theta^{(i+1)}(\chi_i a_i) \end{cases}, \quad i=1,2,3,4 \tag{7}$$

where tangential magnetic field components $\tilde{H}_\theta^{(i)}$ are defined by tangential electrical field components as

$$\tilde{H}_\theta^{(i)}(r) = \frac{j\omega\varepsilon_i}{\chi_i^2}\frac{\partial E_z^{(i)}(r)}{\partial r} \tag{8}$$

Matching conditions (7) consist of four pairs of equations. This system (7) can be solved consecutively: the first pair of equations that contains unknown parameter F_1 is solved with respect to F_2 and G_2. Substituting these coefficients into the next pair of equation, the coefficients F_3 and G_3 are obtained as linear parametric expressions with respect to parameters F_1 and so on. The last pair of equations is now the system of linear equations with respect to unknown parameters F_1 and F_5. In particular, the solution for the coefficient F_1 in ultra-relativistic case ($v=c$, $\tau \to 0$) is given by:

$$F_1 = -G_1 + G_1 a_1^2 U^{-1} \tag{9}$$

where

$$U = a_2^2 - 2\frac{a_2\varepsilon_3}{\chi_3\varepsilon_0}V \tag{10}$$

with

$$V = \frac{\varepsilon_3\chi_4 R_4(a_3)S_3'(a_2) - \varepsilon_4\chi_3 R_3'(a_2)R_4'(a_3)}{\varepsilon_3\chi_4 R_4(a_3)S_3(a_2) - \varepsilon_4\chi_3 R_3(a_2)R_4'(a_3)}.$$

In above expression

$$R_i'(r) = K_0(\chi_i a_i)J_1(\chi_i r) + J_0(\chi_i a_i)K_1(\chi_i r)$$
$$S_i'(r) = -K_1(\chi_i a_i)J_1(\chi_i r) + J_1(\chi_i a_i)K_1(\chi_i r)$$

The longitudinal electrical field component in the beam region $0 \le r \le a_1$ is then presented as:

$$\tilde{E}_z^{(1)}(r) = \left(-G_1 + G_1 a_1^2 U^{-1}\right)I_0(\tau r) + G_1$$

that for ultrarelativistic case ($\tau \to 0$, $I_0(\tau r) \to 1$) is modified to:

$$\tilde{E}_z^{(1)}(r) = G_1 a_1^2 U^{-1} = qU^{-1}je^{-jkz}/c\pi k\varepsilon_0 \tag{11}$$

Expression (11) is independent from a_1 and therefore is valid for the point like charge. The monopole longitudinal impedance is then:

$$Z(k) = -jZ_0 U^{-1}/\pi k \tag{12}$$

with $Z_0 = 120\pi\ \Omega$ the impedance of free space.

SPECIAL CASES

For the tube with finite wall thickness without cover $a_2 = a_3$ the expression for U simplified to

$$U = a_3^2 - 2\frac{a_3}{\varepsilon_0}\frac{\varepsilon_4 R_4'(a_3)}{\chi_4 R_4(a_3)}. \tag{13}$$

For the tube with infinite wall thickness ($a_4 \to \infty$) and without cover we get

$$U = a_3^2 - 2a_3\frac{\varepsilon_c vH_1^{(1)}(va_3)}{k^2(\varepsilon_c - \varepsilon_0)H_0^{(1)}(va_3)}, \tag{14}$$

where $H_{0,1}^{(1)}(vb)$ are the Hankel functions of the first order and $v = \sqrt{-j\mu_0\sigma_4\omega}$ is the radial propagation constant.

An expression (14) is the most general form of the infinite resistive tube impedance, obtained by Chao [2].

In the case of thick $(d = a_3 - a_2 << a_3)$ cover with low conductivity $(\sigma_3 << \sigma_4)$ one can write:

$$U = a_3^2 + 2\frac{a_3\varepsilon_4}{\chi_4\varepsilon_0}\left\{\frac{\sigma_3}{\sigma_4} + \frac{s_0^2}{a_3^2}\frac{1 - \frac{\sigma_3}{\sigma_4} + \frac{d}{a_3}}{\frac{s_0^2}{a_3^2} + (1+j)\sqrt{\kappa}\frac{d}{a_3}}\right\}, \tag{15}$$

where $s_0 = \left(2ca_3^2\varepsilon_0/\sigma_4\right)^{1/3}$ is a characteristic distance for the thin part of the tube and $\kappa = ks_0$ is a dimensionless wave-number.

NUMERICAL EXAMPLES

The numerical calculations of two-layer tube impedance for the different thickness of cover are shown on Fig.2. The cover (NEG) material conductivity $\sigma_3 = 5.5\cdot10^4\Omega^{-1}m^{-1}$ is negligibly small with respect to the main tube copper conductivity $\sigma_4 = 5.88\cdot10^7\Omega^{-1}m^{-1}$. Tube inner and outer radii are equal to $a_2 = 1.85mm$ and $a_4 = 2mm$ correspondingly. The solid curves on the picture show the infinite thickness homogeneous tube impedances with wall material conductivity σ_3 (left) and σ_4 (right); the inner radius is a_2. The dashed curves present the impedance dependence from the thickness of the cover. There are 6 dashed curves on the graphic that correspond to the cover thickness of 10, 2, 1 μm and 100, 10 and 1 nm.
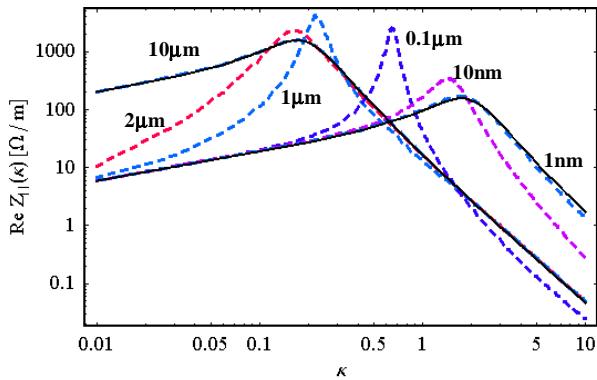
Figure 2. Real part of two-layer (copper-NEG) tube impedance versus cover thickness, $\sigma_3 < \sigma_4$

As it follows from the Fig. 2, the two-layer tube impedance curve is intermediate between two limited infinite thickness tube impedances. In discussed case of cover low conductivity the low-frequency part of impedance tends to cover material tube impedance, and the high frequency part tends to the main tube material impedance. The resonant frequency of the impedance is shifted to the high frequencies for the thinner cover and reaches the main tube material impedance for the very thin cover.

Fig.3 presents the impedance of the stainless-steel (SS) tube $\left(\sigma_4 = 0.14 \cdot 10^7 \Omega^{-1} m^{-1} \right)$ with the copper $\left(\sigma_3 = 5.88 \cdot 10^7 \Omega^{-1} m^{-1} \right)$ cover. Here we have an inverse effect: with the cover depth decreasing the resonant frequency is shifted from the copper tube impedance resonance to the stainless-steel resonance.
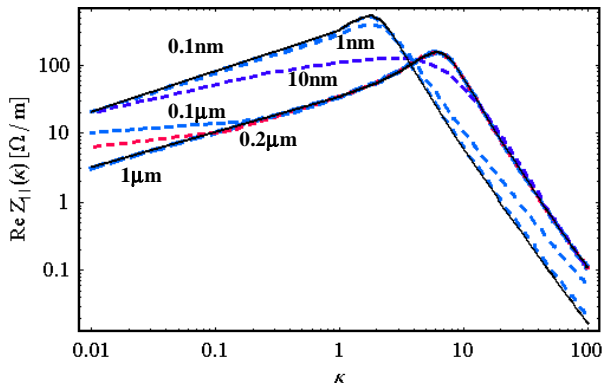

Figure 3. Real part of two-layer (SS-copper) tube impedance versus cover thickness, $\sigma_3 > \sigma_4$
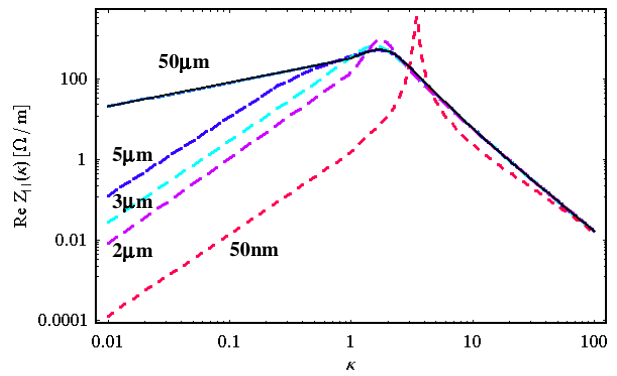

Figure 4. Impedance dependence versus wall thickness

The main conclusion is: the two-layer tube impedance is equal to impedance of tube from the layer material at frequency region where the skin depth is much larger than cover thickness and coincides with the main tube material impedance for the frequencies at which the skin depth of the cover is much less than the cover thickness. In the intermediate region, when there is essential difference between two materials conductivities, the impedance growth at the shifted resonance frequency is observed.

On the Fig.4 the dependence of the impedance of the stainless-steel tube from the wall thickness is presented. Inner wall radius is equal to 1.85mm, as before. Outer radius varies from 50μm up to 50nm. Dashed curve is the real part of impedance of stainless-steel tube with infinity wall thickness. As it follows from the figure, the finite thickness of the tube up to the 50 μm does not affect the tube impedance. Further decreasing of thickness results to total impedance decreasing.

CONCLUSION

The impedance for the two-layer tube with finite wall thickness is obtained. The result is an exact analytical solution for the ultra-relativistic case, applicable for any two-layer tube with arbitrary material and thickness. The formula generalized Chao's formula for the homogeneous tube with infinite wall thickness. The numerical examples for different two-layer tubes are given.

REFERENCES

[1] B.W. Zotter and S.A. Kheifets, "Impedances and Wakes in High-Energy Particle Accelerators," Singapore, World Scientific, 1997.

[2] A.W. Chao, "Physics of Collective Beam Instabilities in High Energy Accelerators," New York, John Willey & Sons, Inc., 1993.